Anomalous Loss Mechanisms in High Purity Nb Cavities

R.W.Röth, V.G.Kurakin, G.Müller, H.Piel, J.Pouryamout, D.Reschke, N.Tellmann
Fachbreich Physik, Bergische Universität Wuppertal, Germany

Abstract

Although the acceleration gradient and the residual surface resistance of niobium cavity resonators could significantly be improved by the use of high purity material and optimized cleaning techniques, the fundamental material limits are still not reached yet. This paper summarizes some results of our investigation on local defects, hydride precipitation, lossy oxides and similar anomalities. Detector systems for x-ray mapping and thermometry in superfluid helium allow locally resolved investigation of the dependence of these losses on the amplitude and frequency of the rf field.

Introduction

Superconducting linear accelerators for electrons in the TeV regime (TESLA) need cavities with acceleration gradients of E_{acc}= 15 - 30 MV/m [1]. To achieve this performance reliably, field emission loading has to be overcome, first [2]. Likewise important, a small surface resistance is necessary to provide thermal stability at high field strengths [3] and to allow for acceptable cryogenic costs. Obviously, this can only be achieved, if the Q_0 at low field is already high and does not drop significantly with increasing field amplitude. Therefore, the density and size of local defects has to be small. In addition, for cavities operating above 500 MHz, a better understanding and control of the homogeneous part of the residual surface resistance R_{res} is necessary.

I. Magnetic and dielectric surface resistance: local distribution and field dependence

Most of our investigations on the residual surface resistance of niobium of different purity were performed with single-cell cavities. Fig.1a shows a typical $Q_0^{res}(E_{acc})$-characteristic of a postpurified 3-GHz-cavity with RRR ≈ 200, measured at T_b = 1.6 K. Though the cavity developed no detectable field emission up to the thermally induced quench at H_p = 103 mT (E_p = 63 MV/m), the unloaded quality factor reduces with increasing field strength. The surface resistance $R_{res} = G/Q_0^{res}$ fits nicely to

$$R_{res}(H) = R_{res}(0) + \alpha \cdot H^2 \qquad (1)$$

(Fig.1b). This dependence is observed very often (e.g. Figs.3b, 6). It may originate from surface impurities that strongly increase their resistance when they are heated in the rf surface field. Another proposed explanation assumes defects with a pointlike contact to the niobium wall, having a nearly constant surface resistance (e.g. welding beats, delaminations, cavitations in the surface). Such defects can become very hot. With increasing field strength, the superconducting Nb in their vicinity is heated signifi-

cantly, and the local surface resistance $R_s^{loc} = R_{BCS}(T_b+\Delta T) + R_{res}^{loc}$ becomes dominated by its exponentially increasing BCS-part. Thus, a strongly growing region of increased losses is introduced.

For both interpretations, the slope α of the $R_s(H)$-increase (eq.1) is expected to grow with the size, the number, and the resistance of the defects. However, α is expected to reduce, if the RRR of the niobium is improved (see Fig.6, S3-5 and S3-8). To proof these expectations, detailed model calculations are under way, taking the temperature dependence of the thermal conductivity $\lambda(T)$ and the BCS-losses $R_{BCS}(T)$ into account.

Quantitative information about the local distribution and the field dependence of the residual surface resistance can be obtained with our thermometry in superfluid helium [4,5]. At first, a temperature map with complete spatial resolution is measured with a set of scanning thermometers. In a second cryotest other thermometers can be glued to the cavity wall with Apiezon-N grease, at all positions of interest. These fixed thermometers are well calibrated:

$$\Delta T = \eta(T_{bath}) \cdot R_K \cdot \{ dP/dA \}^{\alpha} \qquad (2)$$

where

$$dP/dA = \tfrac{1}{2} \cdot R_s \cdot H^2 + \tfrac{1}{2} \cdot \frac{\varepsilon_0}{\mu_0} \cdot R_E \cdot E^2 \qquad (3)$$

and the measured efficiency $\eta(1.5K) = 0.30 \pm 0.08$, $\alpha = 1.02 \pm 0.05$, and $R_K = 7.6\,cm^2 \cdot K/W$ for the Kapitza resistance [4]. Close to the equator, where $E = 0$, eq.(2) simplifies to

$$\Delta T = \tfrac{1}{2} \cdot \eta \cdot R_K \cdot R_s^{loc}(T_{wall}) \cdot H^2 \qquad (4)$$

Fig.1c-f present an example of such a measurement series, taken at 1.6 K just below the quench limit in the experiment discussed above. Obviously, only one defect close to the equator has dominated the power consumption of this cavity (Fig.1c). With the fixed thermometers, the temperature of the cavity wall close to this defect was found to increase exponentially with the magnetic surface field - at least above $E_{acc} = 12\,MV/m$ ($H_p > 50\,mT$) (Fig.1d). According to eq.(4), the superconducting niobium in the surrounding of the defect is heated to temperatures, where $R_s(T_{wall})$ is dominated by its exponentially increasing BCS part ($T_{wall} = T_{bath} + \Delta T$; $\Delta T \sim H^2$).

In the defect-free areas near to the equator, eq.(4) is satisfied with a constant local surface resistance of $R_s^{loc} = 4.2 \pm 1\,n\Omega$ (Fig.1e). This value nearly fits the BCS-surface resistance at the given bath temperature of 1.6 K. Thus, most of the cavity surface shows no significant magnetic residual surface resistance. If R_s^{loc} were spread homogeneously over the cavity surface, a $Q_0^{res} = 7 \cdot 10^{10}$ would have resulted up to the maximum field strength of about 100 mT. However, the residual Q_0 is already loaded to $Q_0^{res} = 10^{10}$ at low field level and decreases further as H increases. Both has to be attributed in part to the local defect and to dielectric losses.

Evidence for homogeneously distributed dielectric losses can be derived from the temperature signals ΔT, measured along two defect-free meridians. In Fig.1f, the corresponding local heat-flux density dP/dA (resulting from eq.(2)), is compared to the value, merely expected from the distribution of the local magnetic surface field $H^{loc}(s)$. (dashed line; s-parameter: see Fig.2f). A least-square fit (solid line) to eq.(3) yields a dielectric residual resistance of $R_E = 2.4 \pm 0.7\,n\Omega$. At low field strengths, it is responsible for about 30% of the residual losses.

II. Losses due to hydride precipitation: local distribution, temperature and frequency dependence

Cavities, made from high purity niobium (RRR > 150), may show a significant increase of their surface resistance, when they are stored at temperatures around 100 K for several hours [6]. In 1.5-GHz-cavities, a reduction of the quality factor at 1.5 K by more than three orders of magnitude has been observed. This effect disappears completely after a temperature cycle to $T \approx 300$ K, followed by a sufficiently fast cooldown to below 77 K [2]. In 1989, the formation of lossy hydride particles by the precipitation of interstitially dissolved hydrogen gas was suggested as source of the additional losses [2]. This hypothesis is well accepted meanwhile, and the properties of the NbH_x-system are under investigation. In addition to the review article concerning hydride precipitation in niobium [6], some interesting results of our experiments are summarized in Fig.2a-f in more detail.

Fig.2a presents the temperature dependence of the surface resistance of a hydride contaminated 1.5-GHz-cavity (RRR ≈ 180). Obviously, it is not possible to describe the losses, increasing the BCS surface resistance of the pure niobium ($R_s^{BCS}(4.2\,K, 1.5\,GHz) \approx 0.75\,\mu\Omega$) by a constant residual resistance R^{res}. On the contrary, the data can be fitted to $R_s(T) = A/T \cdot \exp(-\Delta/kT) + R^{res}$, where $R^{res} = 0.85\,\mu\Omega$ ($Q_0^{res} = 3 \cdot 10^8$), and $\Delta/kT_c = 1.20$ (assuming $T_c = 9.2$ K). Maybe, an additional superconducting transition takes place at about 2.2 K. To check this, additional experiments are needed. Nevertheless, the properties of the superconducting niobium are changed completely.

In another 1.5-GHz-cavity (RRR ≈ 300), slowly warmed from 4.2 K to about 150 K, the unloaded quality factor at 1.4 K dropped to only $2 \cdot 10^7$. A fast cooldown of the same cavity yielded a residual $Q_0^{res} = 10^{10}$, either before and after the experiment discussed here [2]. A temperature map of the loss distribution in the hydride contaminated case is presented in Fig.2b. The map was taken in subcooled helium ($T_b = 3.8$ K) at $E_{acc} = 0.8$ MV/m in the TM_{010}-mode. It proves, that the hydride precipitation causes a nearly homogeneous surface resistance. The local maxima at the bottom side of the irises originate from a reduced cooling, due to the horizontal mounting of the beam tubes (Fig.2f). However, the maximum close to the upper equator region must be

explained with a larger size or concentration of hydride particles. Because this enhanced loss appeared at the highest part of the cavity in the cryostat, it may be caused by a different cooling and warming speed, there.

Comparing the ΔT-signals measured along all meridians with the local distribution of the corresponding squared local magnetic surface field $H^2_{loc}(s)$, the existence of enhanced losses in the iris region can be assumed. Evidence for dielectric losses was obtained in an experiment with another 1.5 GHz cavity after slow cooling from room temperature with about 2 K/h. Figs.2c and 2d show the temperature increase at the bottom meridian in the rotational symmetric modes TM_{010} (1473 MHz) and TE_{011} (2853 MHz) at different field strength in comparison to the expected (normalized) loss distribution. Obviously, a local maximum caused by enhanced hydride concentration was present at the bottom of the cavity. After subtraction of the local peak, dielectric losses, similar to those of Fig.1f, are necessary to explain the enhanced heating at the iris in the fundamental mode.

The dependence of the hydride-induced losses on the surface magnetic field H_s was investigated at the local maximum near the equator (Fig.2e). In both modes, the temperature signal increases proportional to H_s^2

$$\Delta T = c \cdot R_s(\omega) \cdot H_s^2 \qquad (5)$$

$$R_s(\omega) = c^* \cdot \omega^{\alpha} \qquad (6)$$

Comparing the slope $c \cdot R_s(\omega)$ in both modes and normalizing them with respect to frequency yields $\alpha = 1.8 \pm 0.4$. This result supports the model calculation [6], predicting a square law frequency dependence of the hydride induced surface resistance.

III. Residual losses due to adsorbed gases

In most of our experiments, an increase of the residual surface resistance is observed, after quickly flooding the evacuated liquid helium vessel with room temperature helium gas, to bring the superfluid bath to subcooled conditions at normal pressure. As soon as the warm gas hits the stainless steel pumping tube of the cavity UHV system in the cryostat, the cryopumped residual gases inside are set free. Because the pumping speed of the small Ti getter-pump (outside the cryostat) is small compared to that of the cold cavity surface, most of the desorbed gases are cryopumped inside the cold cavity.

A nice example of the effect is given in Fig.3a, presenting a test series with a 3-GHz-cavity (RRR ≈ 200), free of detectable field emission up to the thermal quench at $H_p \approx 103$ mT. As usual, the best performance was obtained initially after a fast cooldown from room temperature to 1.5 K (curve 1). After the experiment was interrupted by too low a level of sf helium, the cryostat volume was flooded with warm helium gas, as described above. Refilling liquid helium and puming again to 1.5 K, the next day, the quench field strength was reproduced, but the residual resistance had

increased by a factor of about 4 (curve 2). To check, that this was due to adsorbed gases, the cavity was warmed up, stored and pumped at room temperature for 72 h, and tested again. As expected, the residual quality factor recovered partially (curve 3).

In all three tests, the surface resistance increases proportionally to the square of the surface field (eq.(1)). Normalized to the minimum residual resistance ($R_s(0) - R_{BCS}$), the additional losses $\Delta R_s = R_s - R_s(0)$ show the same slope up to $E_{acc} = 15$ MV/m ($H_p =$ 62 mT) (Fig.3b). This means, that the residual losses can be explained by the same mechanism, acting with different strength in each case. It seems, that the different covering of the superconducting surface with residual gases is responsible for the residual resistance, probably even in the best state of the cavity. Thus, to achieve low residual losses, the UHV-system of the cavity has to be baked and the pressure before cooldown must be small.

IV. Field emission loading due to adsorbed gases

Fig.4 presents a set of x-ray- and ΔT-maps, taken at $E_p \approx 22$ MV/m in a 1.5 GHz single-cell cavity (RRR $\approx$ 300). They show the effects of rf- and He-processing as well as cryocycling on the activity of field emitters. According to trajectory calculations, at the given field strength, most of the primary electrons hit the surface close to the emitter, producing the narrow peaks in the x-ray- and in the ΔT-map (Fig.4g) [5]. The scattered and more energetic secondary electrons are responsible for the broad x-ray-peak at the opposite iris. However, because of the low spatial density of the electron bombardment, no significant temperature increase can be detected, there. During the first rf-processing, some weak emitters could be destroyed. However, as usual, stronger emission started at the positions with the next highest $\beta \cdot E_s$ (lower iris at 75°, Fig.4b). After the first cycle to room temperature (no movement of the cavity), a stronger emitter is activated at the opposite iris at 136° (Figs.4c,4g). This electron source, stable to rf-processing with 25 W (cw), could be destroyed by the bombardment with He-ions (Figs.4d,4g). However, a second cycle to room temperature activated (new) emitters in the already processed area (Fig.4e). Again, the emission could significantly be reduced with He-processing (Fig.4f). All these observations show, that the activity of emitters is strongly interfered by adsorbed gases.

V. Influence of standard surface preparation techniques on the residual losses

The optimum surface cleaning method has to be cheap, easy to use, and quick. Most important, it has to yield a very high residual quality factor Q_0^{res} up to the maximum field strengths. Therefore, local defects and field emission sites have to be eliminated, reliably. Today, the relatively simple wet treatment (etching in BCP followed by extensive water rinsing) competes with firing the cavities in a vacuum furnace, especially the solid-state gettering technique. Electropolishing may become an inter-

esting alternative for high frequency cavities (f_0> 1 GHz) in the future. To judge about the potential of the first two methods, some experimentally proven benefits and drawbacks are summarized below.

Residual resistance at low field strength

In accelerator cavities that were never fired, residual resistances down to R_s^{res} = 13 nΩ (Q_0^{res} = $2 \cdot 10^{10}$) can routinely be obtained with chemical etching (BCP) and water rinsing [7–10], if the cooling speed is fast enough to prevent hydride precipitation. To achieve lower losses, the niobium has to be homogenized in a furnace treatment above 1200°C, improving the grain size and reducing the local impurity concentration [2,10]. In our lab, values of R_s^{res} = 3 nΩ (Q_0^{res} = $8 \cdot 10^{10}$) have been obtained in a single-cell 3 GHz cavity (S3-5, Fig.6) [2], after firing for 18 h at 1850°C. Due to the pickup of oxygen, the application of such high temperatures is limited so far to cavities with a low RRR ≈ 40.

For cavities of higher purity (RRR < 700), the solid state gettering protection technique allows the use of temperatures up to 1500°C [2,10]. However, in most of those experiments, where the cavities have been tested without an additional wet surface treatment, the residual resistance is significantly higher than after a usual BCP-treatment (e.g. E5a/E5b, S3-8/S3-13, Fig.6). Though all cavity ports were covered with protecting niobium hats during firing, this may be caused by a contamination of the inner cavity surface with some vapor of the getter material. Fig.5 gives an example of a 3-GHz cavity after single sided titanisation. Obviously, strong dielectric losses (probably due to TiO_2) are introduced, especially at the lower iris. They limited the residual quality factor to only $Q_0^{res} = 2 \cdot 10^7$.

Of course, the niobium covers must not hinder the evacuation of the cavity. Otherwise, residual losses may be caused by the interaction of the cavity surface with the residual gas atmosphere. Thus, the solid state gettering technique has to be optimized with respect to the residual resistance in the future.

Anomalous losses at high field strengths

At high field strength, the dominant field limitation today is still given by the field emission of electrons. Two soures can be distinguished: intrinsic emitters, attatched to the niobium surface (foreign material, geometric irregularities,...), and loose particles (dust, indium,...), both of which may be activated by adsorbed gases. While heat treatment above 1200°C is known to lower the number and activity of intrinsic emitters, the contamination with dust emitters should be prevented by thorough application of rinsing with dustfree water or methanol in combination with a final assembly of the cavities in a clean room.

However, field emission loading could not yet be overcome reliably, even after firing the cavities up to 1500°C [10]. Thus, most of the emission is probably due to a recontamination of the cavity surface with dust particles during assembly or even from the UHV-system of the cryotest setup. Especially the indium seals may play an important role [10]. These results mean in addition, that niobium cavities are not yet limited by intrinsic field emitters, as they were studied in the dc apparatus [7]. Moreover, acceleration gradients of up to $E_{acc} \approx 20$ MV/m can be obtained with chemical etching and water rinsing alone, in single cell cavities (Fig.6), as well as in multicell structures [8,9].

Maybe, if the dust-induced field emission is overcome, firing becomes necessary to destroy the intrinsic emitters and to achieve gradients up to $E_{acc} = 30$ MV/m. Anyway, the recristallisation and homogenisation of the niobium, resulting from a high temperature treatment, is necessary to obtain very low residual resistance values, which are necessary to suppress a global thermal instability (see sections I.-IV.). However, large inclusions of foreign material and small cavitations in the niobium wall cannot be removed in the furnace, even not with firing for 18 h at 1850°C. The only effective remedy against such quench defects is local grinding followed by a local (!) chemical polishing and water rinsing. Then, a final heat treatment may be applied.

Conclusion

Our detailed investigations of the anomalous losses of high purity Nb cavities have shown, that the residual surface resistance at low field levels is caused by several effects. The homogeneous part of the residual losses can partially be attributed to adsorbed and interstitially dissolved gases. Oxide and hydride precipitates change the BCS-characteristics of the niobium and cause magnetic as well as dielectric losses. The frequency dependence of these surface resistances obey $R_s \sim \omega^2$. In our best 3-GHz cavities we proved by thermometry, that the number of localized defects is very small. In the defect-free regions near the equator, the surface resistance comes very close to the BCS value at the operation temperature of 1.5 K. The often observed Q-degradation in field emission free cavities is caused by additional losses in the vicinity of the dominating defects. Thus, at high surface field strengths (even close to the global thermal instability), the quality factor of the cavity is dominated by the few local defects only.

Due to the homogenisation and surface cleaning of the niobium, the smallest surface resistances can be obtained by firing at about 1800°C ($R_{res} \approx 3\,n\Omega$ at 3 GHz). Without protection against oxygen pickup firing of high purity Nb cavities is only allowed for $T \leq 1000$°C. This yields R_{res} values comparable to the result of chemical polishing and rinsing with ultra-pure water ($R_{res} > 10\,n\Omega$ at 3GHz) [11]. Firing a cavity at 1350-1500°C in a protecting Ti-box increases this R_{res} by a factor up to three. Since such

a heat treatment helps to lower the number and activity of (intrinsic) field emitters, the shielding of the cavity interior against Ti vapor has to be improved.

Field emission loading is still the most important limitation for the acceleration gradient - even in cavities, fired above 1200°C and finally rinsed and assembled in a cleanroom. Thus, most of the emission is not yet caused by intrinsic sources but still by particulate matter (e.g. dust), loosely attatched to the niobium surface. Therefore, the contamination control has to be improved. In addition, if the activation of dormant sites by adsorbed gases cannot be prevented, efficient processing techniques are needed.

To provide cavities with high acceleration gradients at low surface resistances, reliably, a better understanding of the adsorption and absorption of gases (e.g. O_2, H_2) by the niobium is necessary. Such investigations have to concern the surface cleaning (interaction with acids, water, and methanol or with the residual gas in a furnace) as well as effects, connected with the residual gas in the cryogenic test site.

Acknowledgement

This work was funded by the German Federal Minister for Research and Technology (BMFT) under the contract number 05 5WT 85 I (7).

References

[1] H.Padamsee (ed.), Proc. of the 1st TESLA Workshop, Cornell, CLNS 90-1029 (1990)

[2] R.W.Röth et al., Proc. of the 2nd EPAC, 1097, Nice 1990, ed. P.Marin, P.Mandrillon

[3] G.Müller, Proc. 3rd Workshop on RF Supercond., ANL-PHY-88-1 Argonne, p.331 (1988)

[4] F.Zobel, Univ. Wuppertal, WU D 89-4

[5] G.Müller et al., Proc. of the 1st EPAC, 1289, Rome 1988, ed. S.Tazzari

[6] B.Bonin, R.W.Röth, review on Q-disesase, this workshop

[7] G.Müller et al., ibid. [5], p. 1292

[8] R.Sundelin, laboratory talk (CEBAF), this workshop

[9] B.Aune, laboratory talk (Saclay), this workshop

[10] H.Padamsee, laboratory talk (Cornell), this workshop

[11] H.Padamsee and G.Müller, Proc. IEEE Part. Acc. Conf., IEEE Cat. Nr.87, CH 2387-9 Washington DC, p. 1833 (1987)

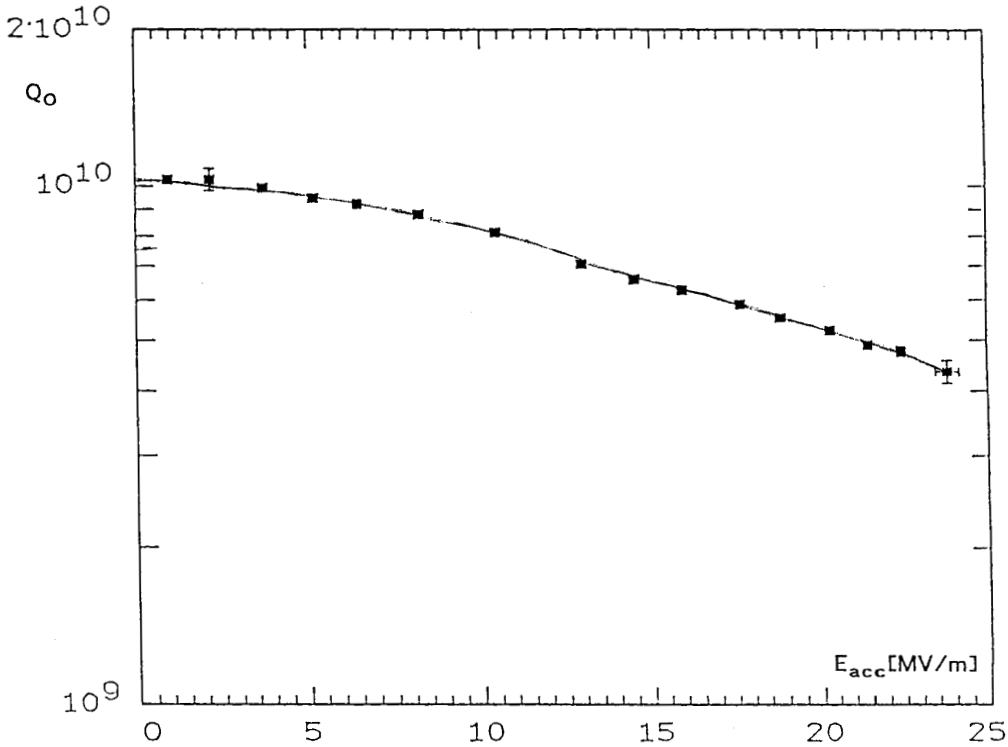

Fig.1a $Q_0(E_{acc})$ performance of a 3-GHz single-cell cavity at 1.5K. No field emission was detectable. Thermal quench at E_{acc}= 24.8MV/m appeared at a local defect.

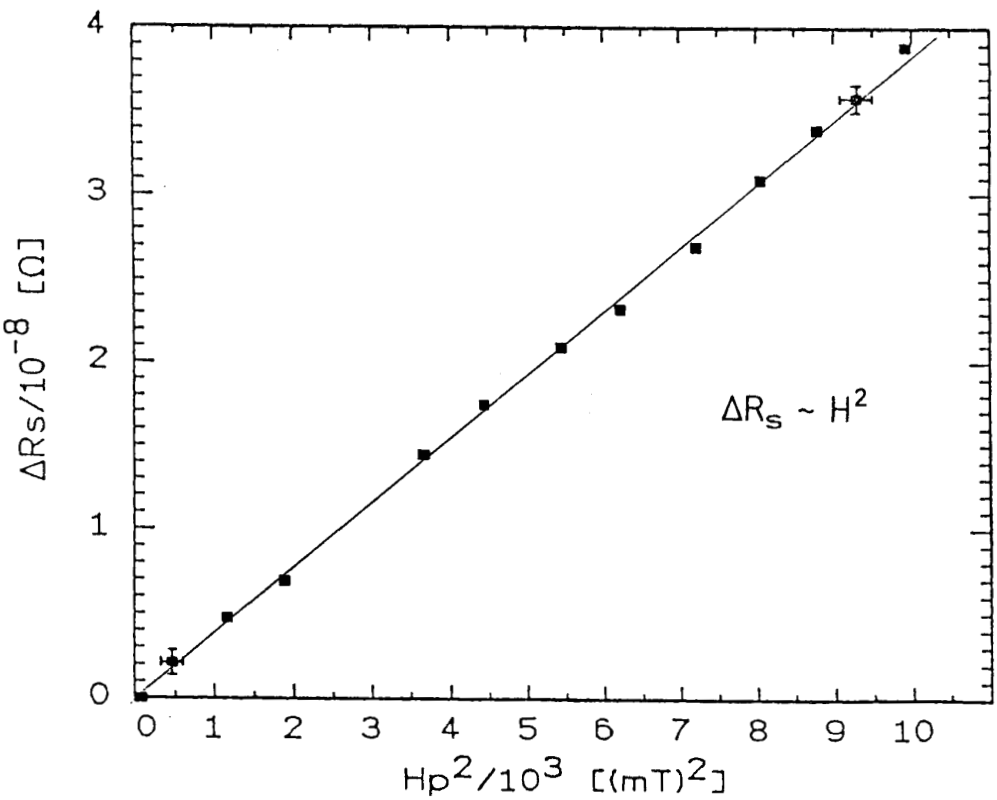

Fig.1b Linear increase of the residual surface resistance $\Delta R_s = R_s(H) - R_s(0)$ with H_p^2.

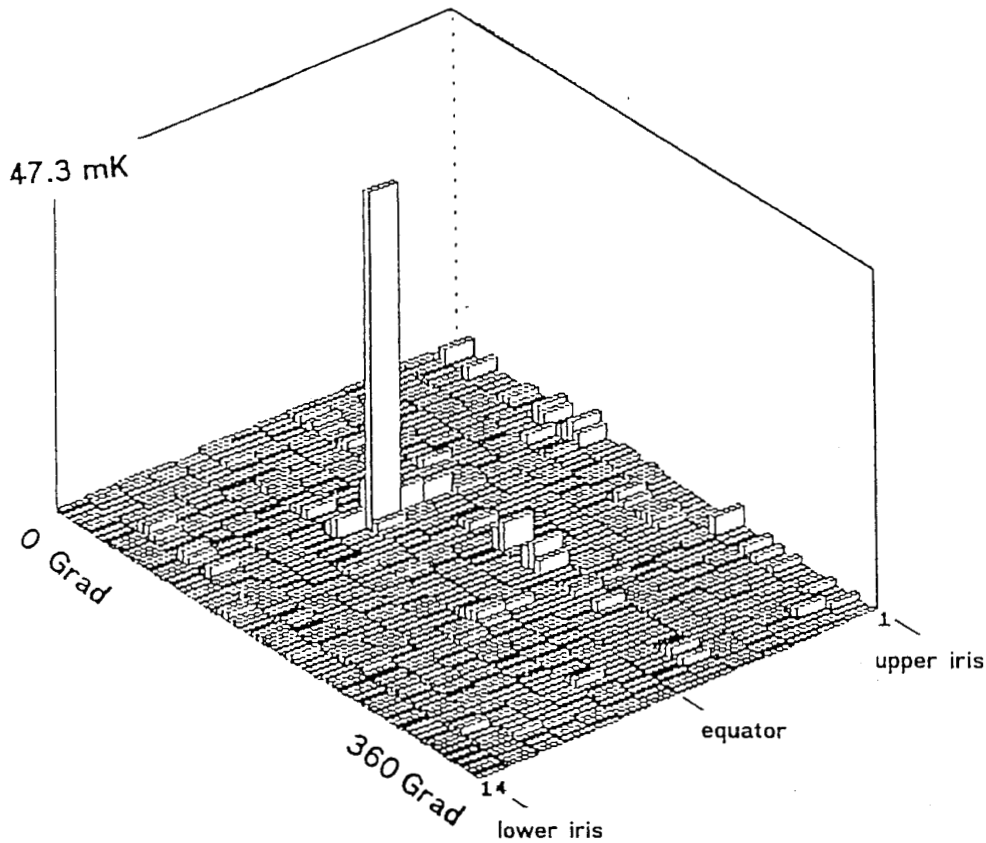

Fig.1c Corresponding temperature map in superfluid helium (1.6 K) at maximum field strength just below the quench (H_p=100 mT). The small signal amplitude is due to the low sensitivity of the movable thermometers.

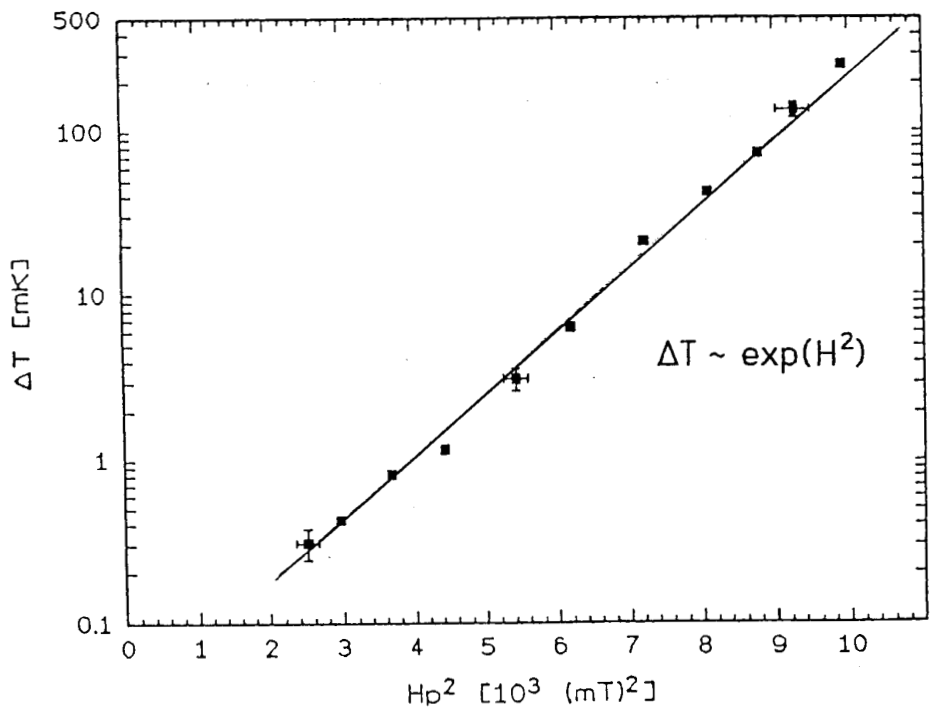

Fig.1d Exponential temperature increase at the local defect near the equator at 1.6 K.

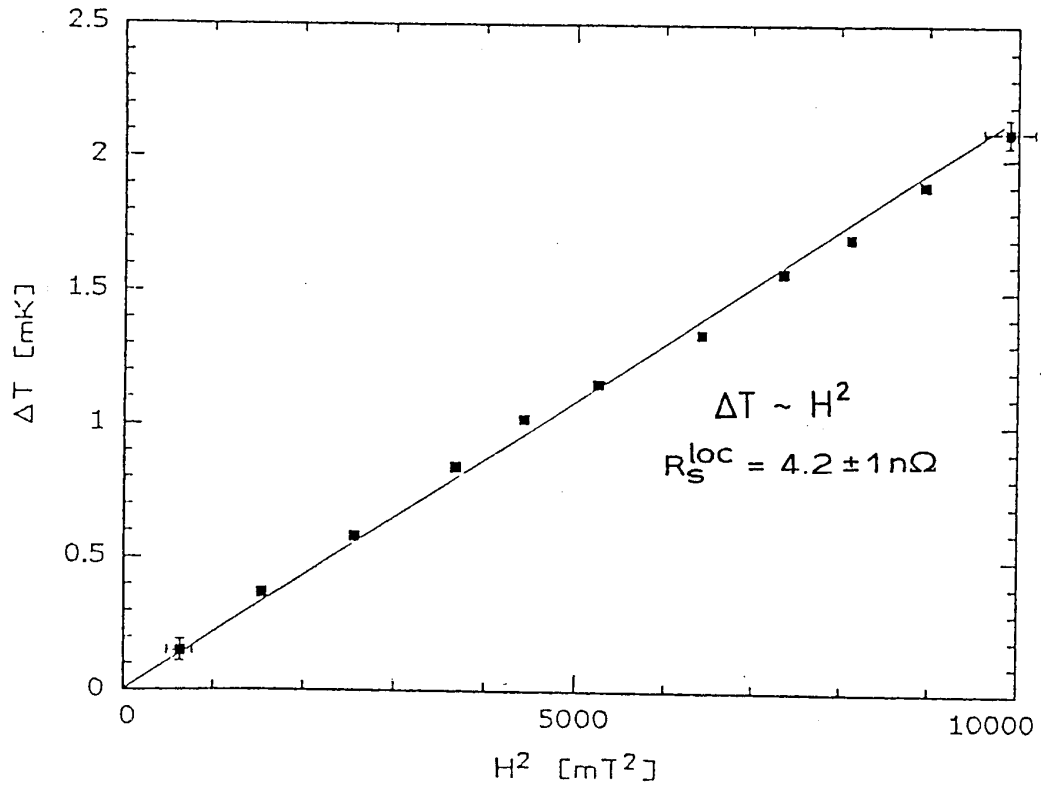

Fig.1e Linear temperature increase at a defect-free surface area at 1.6K.

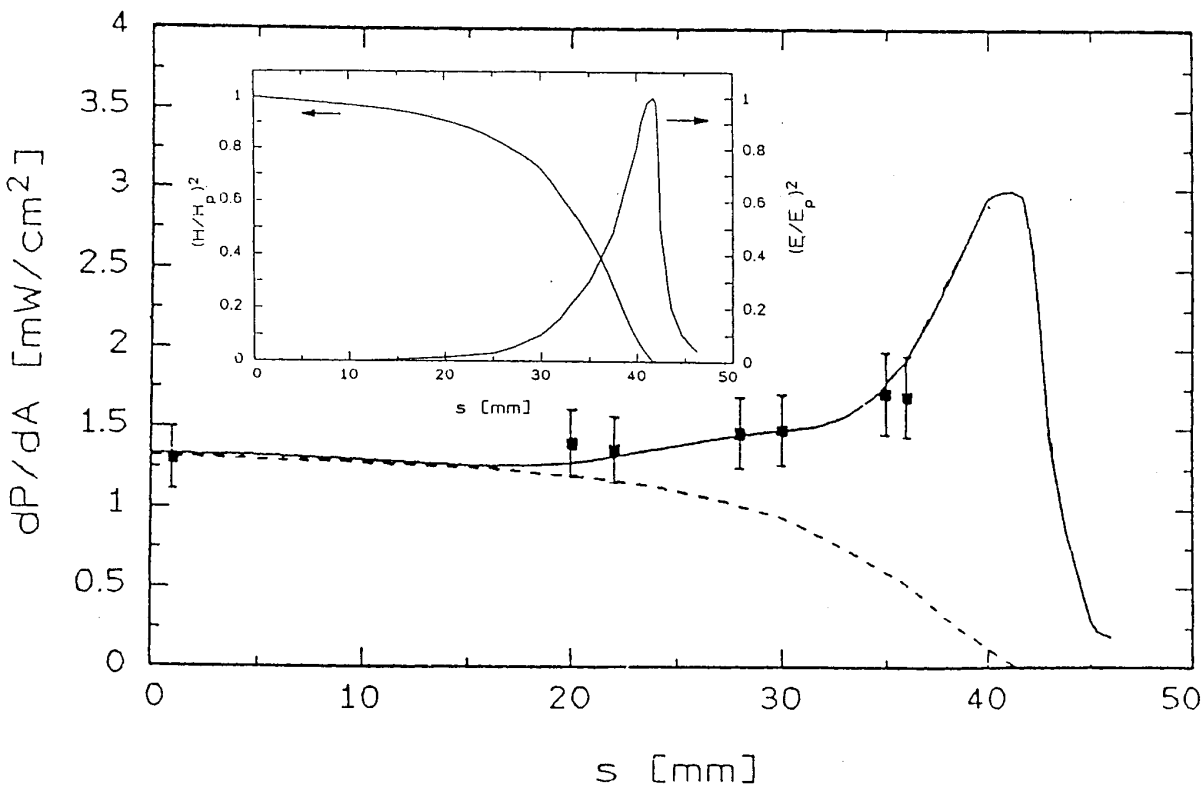

Fig.1f Temperature signals along two defect-free meridians in comparison to the local magnetic and electric field strength show dielectric losses. (s-parameter: Fig.2f)

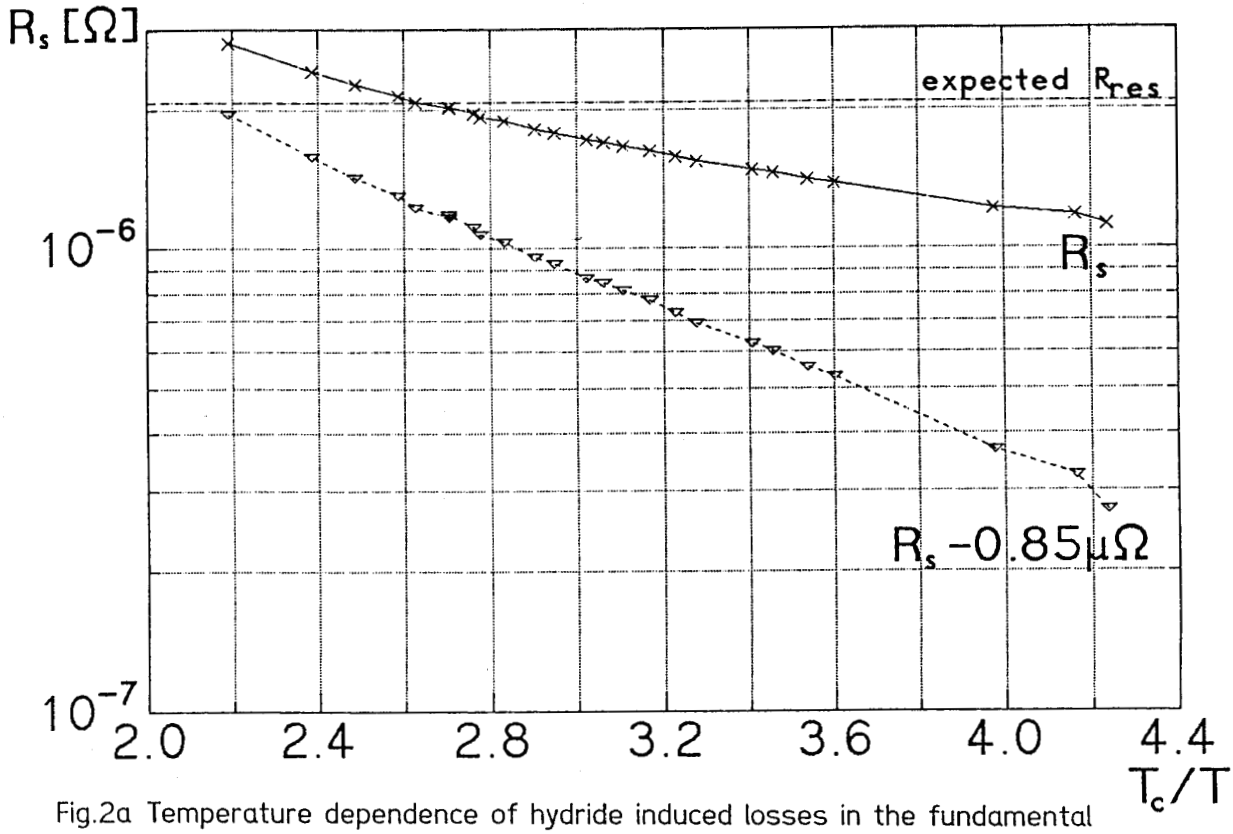

Fig.2a Temperature dependence of hydride induced losses in the fundamental mode at 1.473 GHz. From the quality factor at 4.2K, normally, a temperature independent residual resistance of about 2μΩ would be expected.

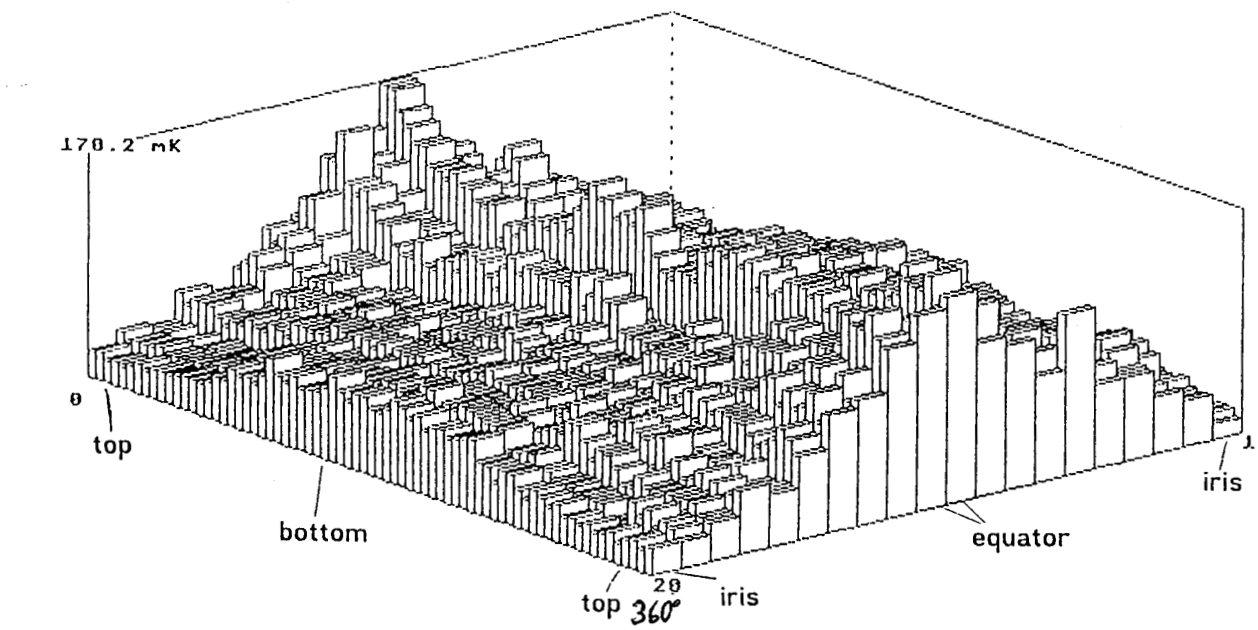

Fig.2b Subcooled temperature map of a hydride contaminated 1.5-GHz-cavity at T=3.8K (E_{acc}=0.8MV/m).

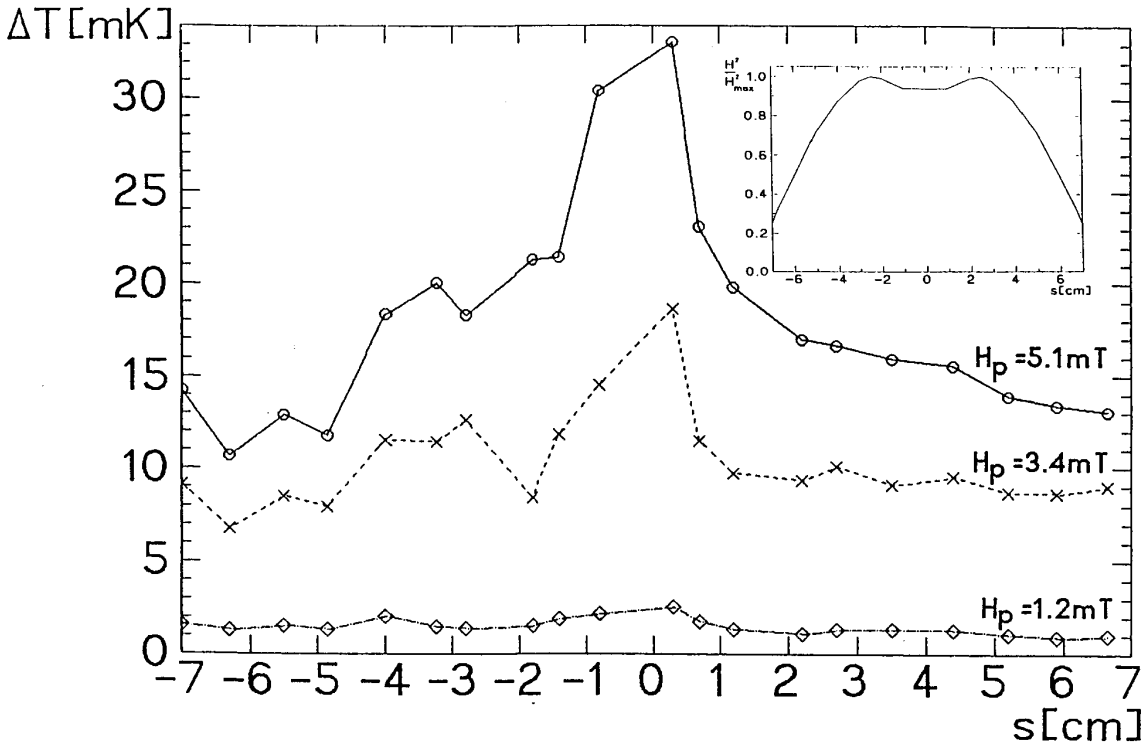

Fig.2c Hydride induced loss distribution at $\varphi = 180°$ and different field strengths in the fundamental mode (TM_{010}, 1.473 GHz). (Subcooled bath at 3.8 K.)

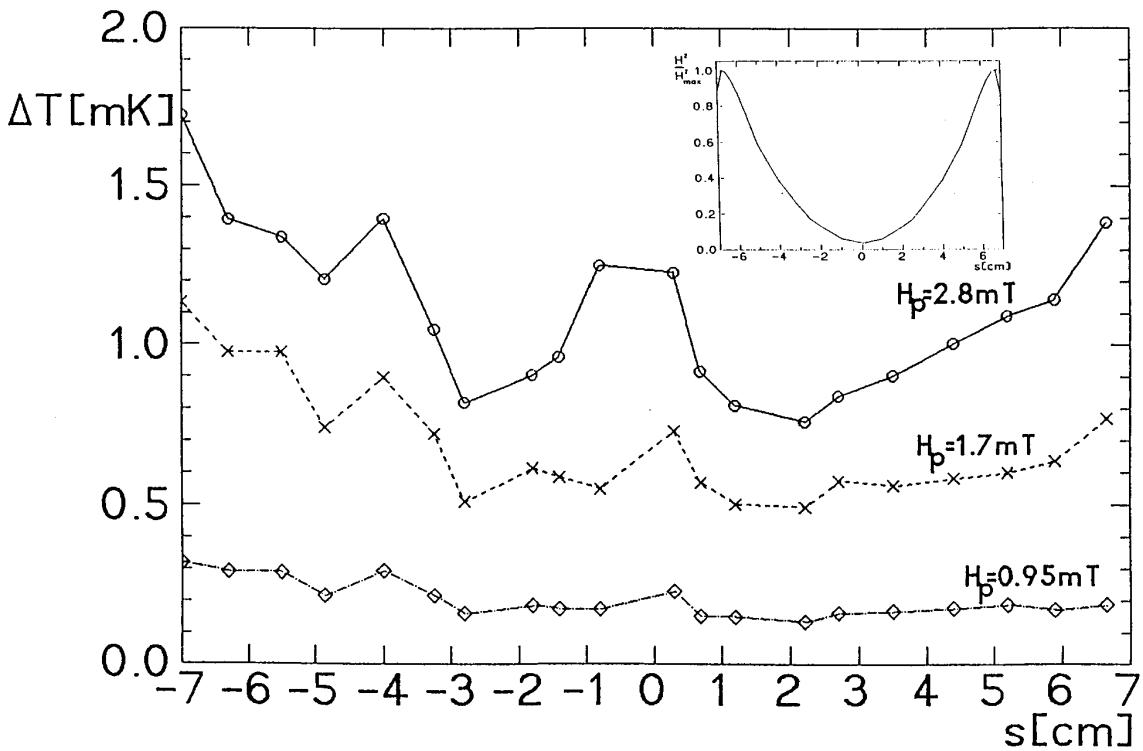

Fig.2d Hydride induced loss distribution at $\varphi = 180°$ and different field strengths in the TE_{011} mode (2.853 GHz), having no electric surface field (3.8 K).

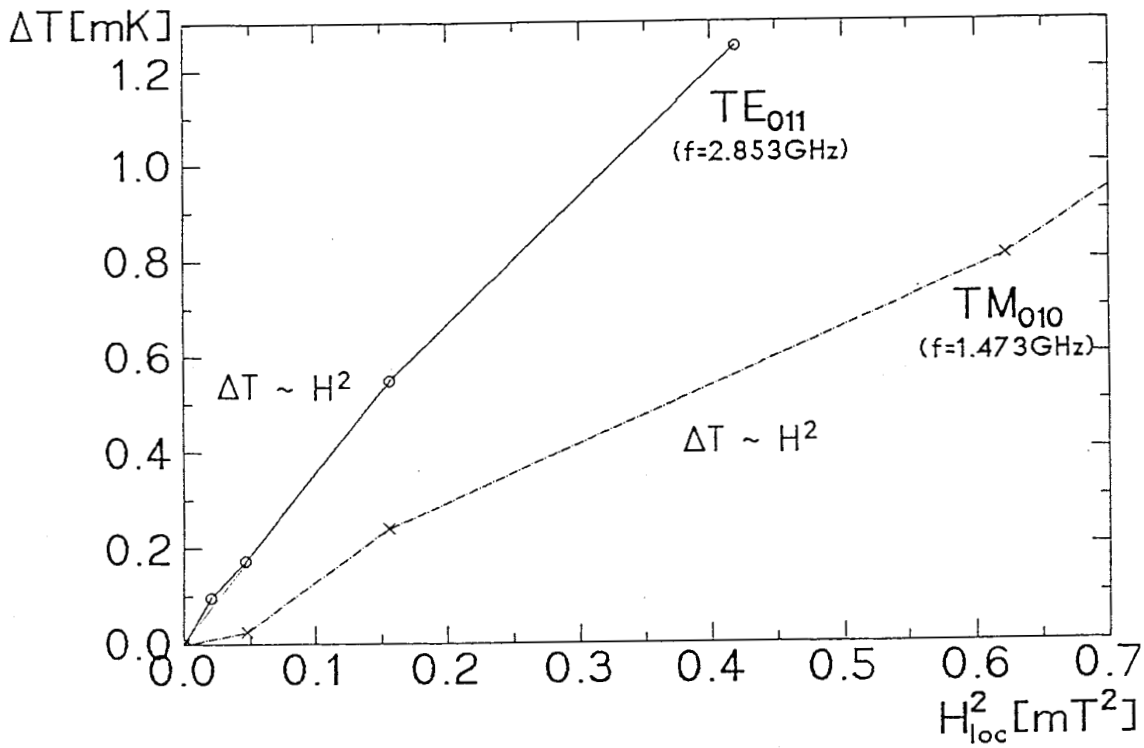

Fig.2e Field dependence of temperature increase at a hydride precipitation.

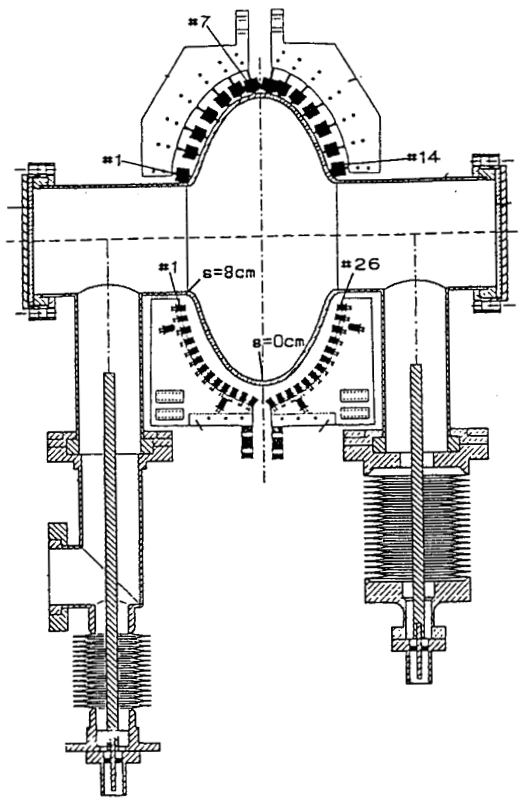

Fig.2f 1.5-GHz-cavity used for the investigations.

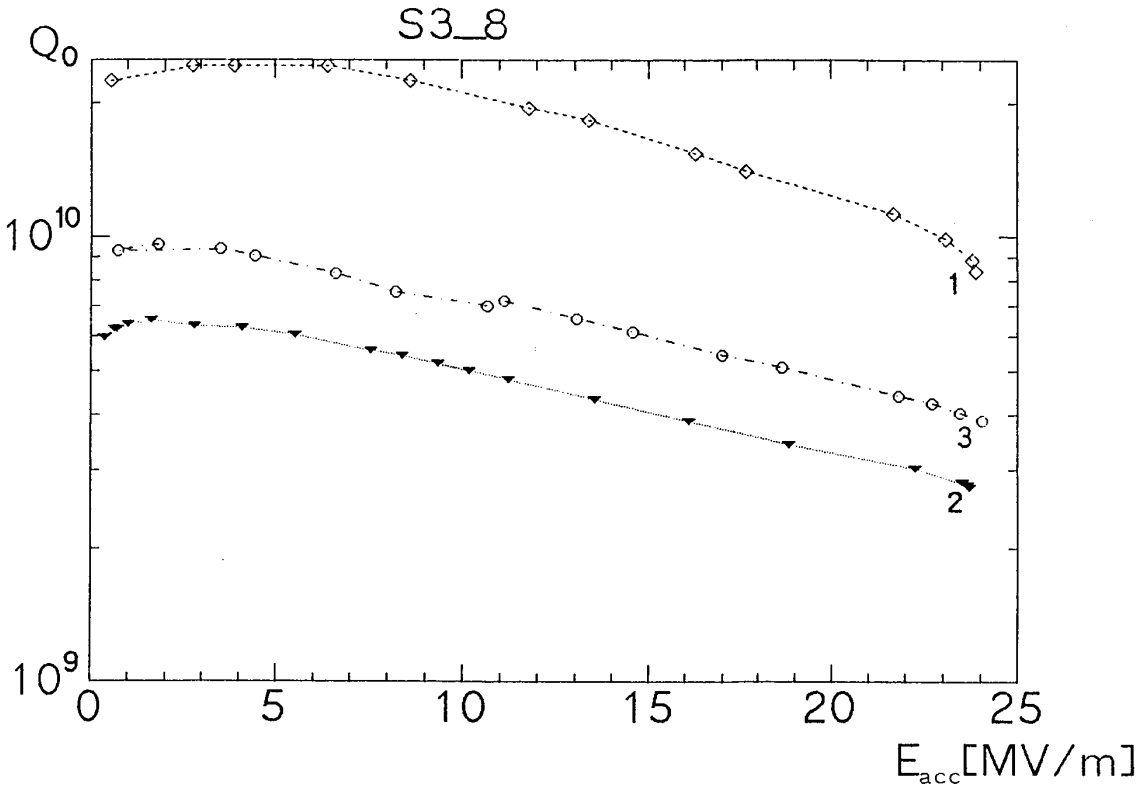

Fig.3a Change of the residual surface resistance of a 3-GHz single cell cavity due to adsorption of residual gases. (1): initial performance, (2): with cryopumped gases, initially frozen in the pumping tube. (3): after cryocycle to 300 K

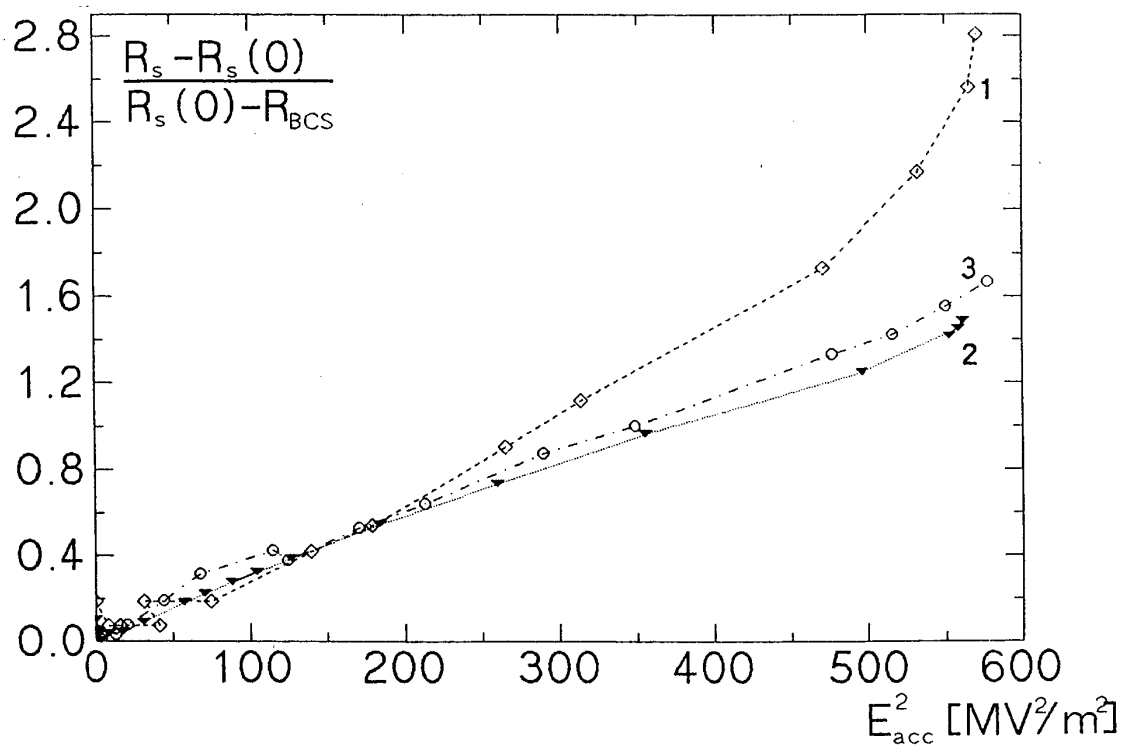

Fig.3b Corresponding $\Delta R_s(E)/\Delta R_s(0)$ versus E^2 plots coincide up to E_{acc}= 15 MV/m.

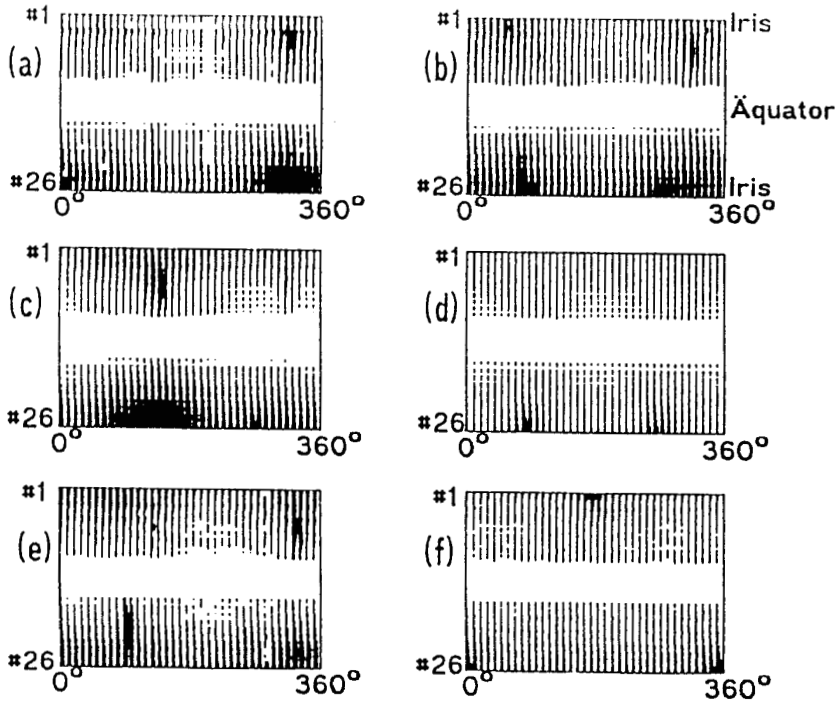

Fig.4 x-ray maps taken at a 1.5 GHz cavity. The darker the area, the higher the intensity. a) initial state, b) after 10 min rf-processing, c) after rt-cycle d) after He-processing, e) after rt-cycle, f) after He- processing again.

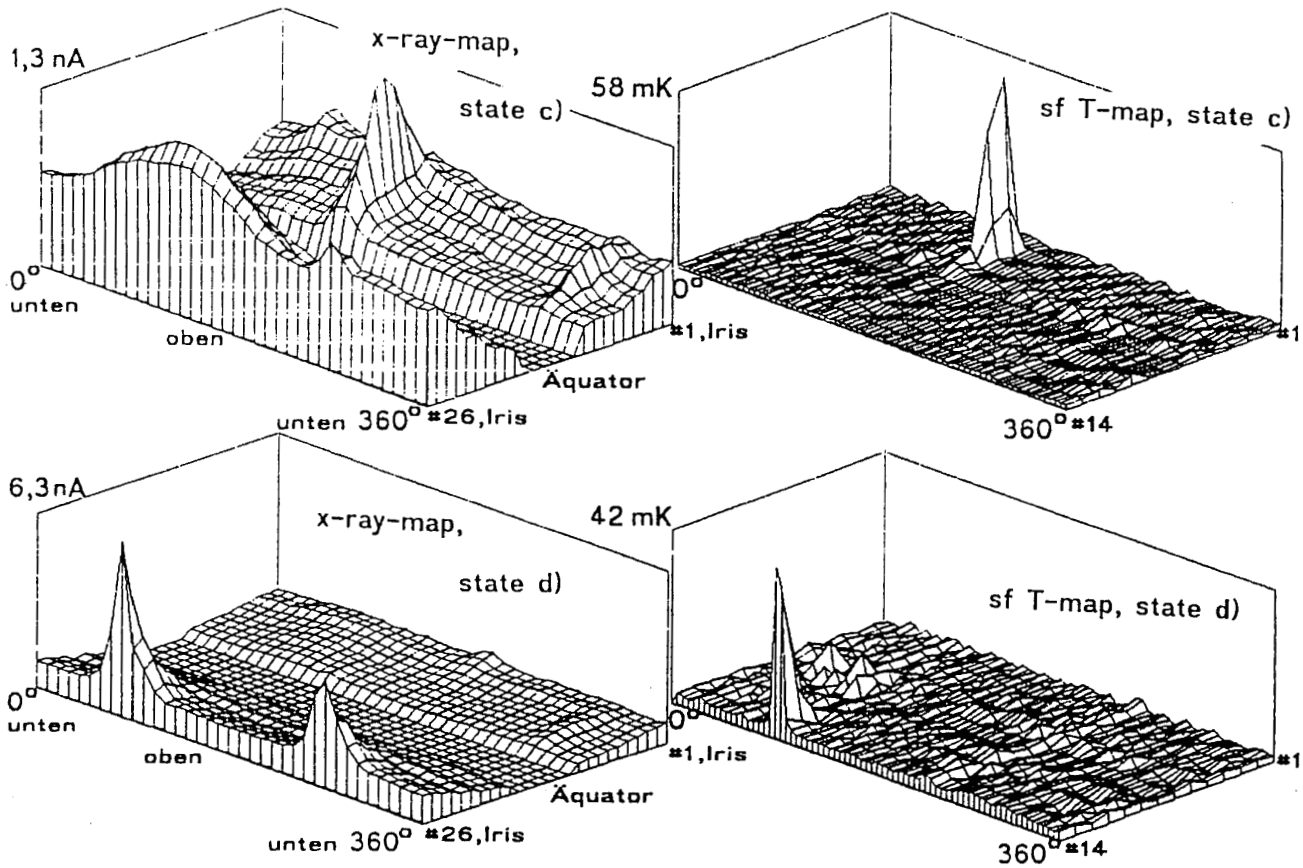

g) 3D x-ray- and sf-temperature maps corresponding to state c) and d)

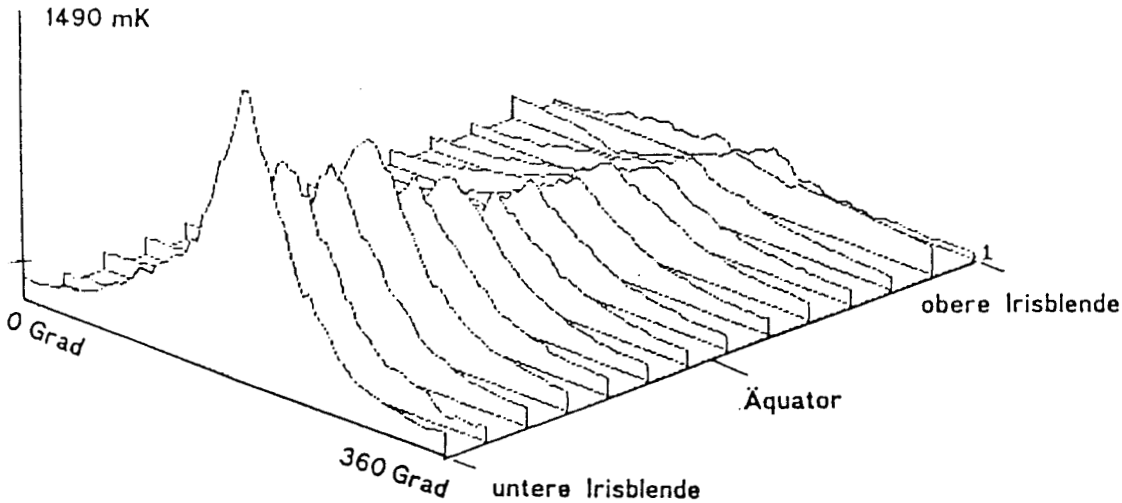

Fig.5 ΔT-map of a 3 GHz single cell cavity in subcooled helium (T= 2.2 K) after firing at 1350°C in a titanium box. Losses are due to TiO_2 ($Q_0^{res} = 2 \cdot 10^7$).

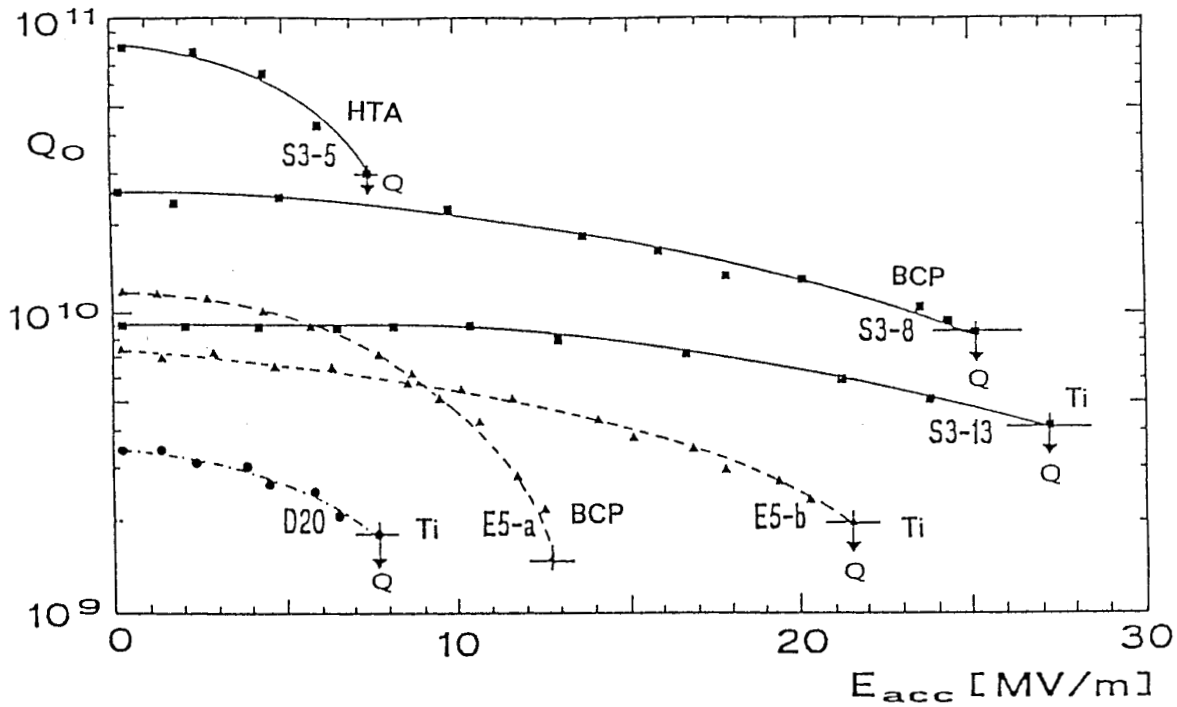

Fig.6 Comparison of the residual losses and fieldemission activity of 3-GHz-cavities after dry and wet surface cleaning. (Dry: firing at about 1800°C without Ti-box (HTA), firing at about 1350°C with Ti-box (Ti). Wet: BCP and water rinsing.)